MINERALOGICAL JOURNAL, VOL. 21, No. 4, pp. 151 - 156, OCTOBER 1999

The structural study on Fe-pumpellyite : An application of Weissenberg technique combined with a synchrotron radiation and an imaging plate

Makio OHKAWA[*], **Setsuo TAKENO**[*], **Akira YOSHIASA**[**] **and Kazumasa OHSUMI**[***]

[*] *Department of Earth and Planetary Sciences, Faculty of Science, Hiroshima University, Higashi-Hiroshima, Hiroshima 739-8526, Japan*

[**] *Department of Earth and Space Science, Graduate School of Science, Osaka University, Toyonaka, Osaka 560-0043, Japan*

[***] *Institute of Materials Structure Science, High Energy Accelerator Research Organization, Tsukuba, Ibaraki 305-0801, Japan*

Abstract

The crystal structure of Fe-pumpellyite from Iwakake, Shimobe-cho, Nishiyatsushiro-gun, Yamanashi Prefecture, Central Japan was investigated by a Weissenberg camera combined with a monochromated synchrotron radiation of wavelength 1.000 Å and an imaging plate. Crystallographic parameters are $a = 8.884(3)$, $b = 5.899(4)$, $c = 19.292(6)$ Å, $\beta = 97.49(3)°$, $A2/m$. The octahedral X-site is larger than the octahedral Y-site. The obtained constrained occupancy ratios of Fe for the X- and Y-sites are 24% and 18%, respectively, i.e., 40% and 60% of total Fe distribute in the X- and Y-sites, respectively.

1. Introduction

Pumpellyite is a well-known rock-forming mineral occurring in low-grade metamorphic rocks such as the pumpellyite-actinolite and prehnite-pumpellyite faces. The general chemical formula of pumpellyite is represented as $W_8X_4Y_8Z_{12}O_{56-n}(OH)_n$. The 7-coordinated W-sites are primarily occupied by Ca and the tetrahedral Z-sites are invariably occupied by Si. The octahedral Y-site is dominantly occupied by trivalent cations, while the octahedral X-site allows for both divalent and trivalent cations (e.g., Mg^{2+}, Al^{3+}, Mn^{2+}, Mn^{3+}, Fe^{2+} and Fe^{3+}).

The basic crystal structure model of pumpellyite was first proposed by Gottardi (1965) and determined by Galli and Alberti (1969). Yoshiasa and Matsumoto (1985) clarified the hydrogen atom positions by the refinement of the structure. These studies were carried out for the Al-rich pumpellyites in which octahedral X- and Y-sites are dominantly occupied by Al^{3+} ions. On the other hand, iron end-member pumpellyite (Julgoldite) was reported by Moore (1971) and Allmann and Donnay (1973). In this structure, the X- and Y-sites are mainly occupied by Fe^{2+} and Fe^{3+} ions.

Pumpellyite and julgoldite form a complete series of solid solutions. Recently, the distribution of Fe ions at X- and Y-sites in the pumpellyite - julgoldite series minerals was investigated by the use of X-ray Rietveld and/or ^{57}Fe Mössbauer methods (e.g., Artioli and Geiger, 1994; Akasaka *et al.*, 1997). However, the structural study using single crystal X-ray diffraction method has not been done yet, because crystal samples of Fe-rich pumpellyite are composed of very fine grains and the crystalline quality of each grain is quite low. In this study, the Weissenberg method combined with imaging plate (IP) and synchrotron radiation as an X-ray source was employed to determine the crystal structure of Fe-pumpellyite. With the application of this method, the data collection for the structure analysis was succeeded on the small single crystal with a low crystal quality.

2. Experimental

A. Specimen

Pumpellyite from Iwakake, Shimobe-cho, Nishiyatsushiro-gun, Yamanashi Prefecture, Central Japan was investigated. Pumpellyite crystals in the locality are found in metabasites forming fine-grained acicular to bladed shapes elongated along the *b* axis. The size of the crystal used for the structure analysis was 20 × 8 × 2 μm^3.

B. Electron-microprobe analysis

Subsequent to the X-ray diffraction experiment, chemical analysis was carried out for the crystal using a JCMA-733II electron microprobe analyzer. Table 1 shows the chemical composition and the number of ions calculated from the analytical data normalized on 32 cations per formula unit. Iron content was estimated by the assumption for all Fe ions to be trivalent. Chemical analyses were also done for several crystals in the same specimen from which the examined crystal was picked out. The compositional variation is shown in Fig. 1 as an Al-Fe-Mg diagram.

C. Diffraction intensity data collection

Diffraction intensity data were collected with synchrotron radiation of the wavelength 1.000 Å which was monochromated by double Si(111) crystals. The wavelength was determined by the diffraction data ob-

TABLE 1. Chemical composition of the pumpellyite used in this investigation.

	wt%		atom
SiO_2	37.55	Si	12.37
TiO_2	0.03	Ti	0.01
Al_2O_3	22.50	Al	8.73
Fe_2O_3	9.64	Fe	2.39
MnO	0.04	Mn	0.01
MgO	1.69	Mg	0.83
CaO	21.68	Ca	7.65
Na_2O	0.01	Na	<0.01
K_2O	0.01	K	<0.01
H_2O (calc.)	5.58		
total	98.73		32

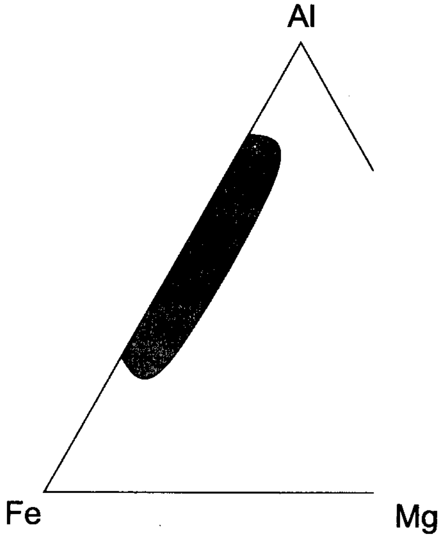

FIG. 1. Solid circle shows the chemical composition of pumpellyite from Iwakake. The shaded area represents compositional variation of the minerals from the same locality

tained from a standard Si powder sample (NBS). A Weissenberg camera method (MAC Science DIP310SOR) was employed at the BL-4B station, Photon Factory, National Laboratory for High Energy Physics, Tsukuba, Japan. The diffraction pattern and intensities were recorded on such a cylindrical IP (400×200mm) of radius 100mm that can cover the range, $-60 < 2\theta < 165°$. To maximize the S/N ratio of the diffraction pattern, the whole equipment was placed in a chamber evacuated to about 6 Pa during the measurements.

The diffraction patterns of several crystals were examined in advance. The reflection spots were always elongated on the IP and their intensities were very weak. The elongation of reflection spot suggests a certain spread of crystal orientation around the *b* axis. The specimen which was used for the data collection is the crystal with the best quality among the examined specimens. Weissenberg photographs were taken with rotation about the *b* axis (layers 0 to 3); ϕ oscillation range of $0 \leq \phi \leq 200°$, ϕ speed of 20°/min and rotation-traverse ratio of 2°/mm. Exposures were varied from 720 to 840 minutes for each measurement. The equi-inclination method was applied to the first through the third layers. Higher layers than third layer could not be taken because of a mechanical limit of the camera. Several oscillation photographs were also taken with various oscillation ranges. Digitizing linear scaled diffraction images of 3200×1600 pixels were outputted by IP reader installed in the diffraction equipment.

Total 213 reflection intensities were detected on the images. All measured reflections were weak and elongated along the ϕ rotation axis (Fig. 2). The reflection intensity within a maximum of 100×100 pixels around each reflection were integrated. The background intensities were also estimated and they were subtracted from the above integrated intensities. The reflection intensities of each layer were scaled with some strong spots on the both oscillation and Weissenberg photographs and were corrected for Lorentz and polarization factors. Lorentz factors were taken from *International Tables for X-ray Crystallography,* Vol. II (1967). Polarization factors were calculated by a equation; $p = 1 - (1 + \cos 2\theta)^2(1 - \cos 2\mu)/(1 + \cos 2\mu)$ assuming a complete horizontal polarized light, where θ and μ indicate Bragg angle and inclination angle, respectively. No absorption correction was applied because the effect was negligible. Experimental conditions are summarized in Table 2.

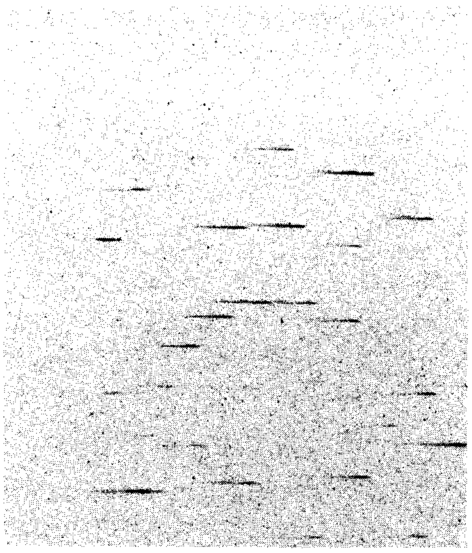
FIG. 2. Weissenberg photograph of 0 layer.

D. Structural analyses

Weissenberg photographs revealed monoclinic symmetry and the systematic absences (*hkl*: $k+l=2n+1$) were consistent with that of the space group *A*2/*m* as

TABLE 2. Crystallographic data and experimental conditions

Crystal system	Monoclinic
a /Å	8.884(3)
b /Å	5.899(4)
c /Å	19.292(6)
β (deg.)	97.49 (3)
V /Å^3	1002.5
Space group	*A*2/*m*
Crystal size (μm)	20 × 8 × 2
Wave length used	Synchrotron (1.000 Å)
Diffractometer	BL-4B Weissenberg camera
Monochromator	Double Si(111)
Start angle (deg.)	0
ϕ oscil. range (deg.)	200
ϕ speed (deg./min.)	20
IP oscil. range (deg.)	100
IP speed (mm/min.)	10
Exposure time (min.)	720 - 840
No. of measured reflections	213
No. of indep. reflections used for refinement	113
R	0.086
R_w	0.083

TABLE 3. Results of atomic positions

Atom	Position	*x*	*y*	*z*
Ca(1)	4*i*	0.244(3)	1/2	0.336(1)
Ca(2)	4*i*	0.190 (3)	1/2	0.155(1)
X	4*f*	1/2	1/4	1/4
Y	8*j*	0.251(2)	0.250(10)	0.494(1)
Si(1)	4*i*	0.055(4)	0.0	0.091(2)
Si(2)	4*i*	0.174(4)	0.0	0.248(2)
Si(3)	4*i*	0.462(4)	0.0	0.400(2)
O(1)	8*j*	0.134(4)	0.213(15)	0.065(2)
O(2)	8*j*	0.267(5)	0.220(13)	0.246(3)
O(3)	8*j*	0.360(4)	0.232(16)	0.413(2)
O(4)	4*i*	0.126(9)	1/2	0.440(4)
O(5)	4*i*	0.122(10)	0.0	0.460(4)
O(6)	4*i*	0.367(10)	1/2	0.041(5)
O(7)	4*i*	0.369(10)	0.0	0.034(5)
O(8)	4*i*	0.045(8)	0.0	0.178(4)
O(9)	4*i*	0.489(11)	1/2	0.180(5)
O(10)	4*i*	0.068(8)	0.0	0.317(4)
O(11)	4*i*	0.503(11)	1/2	0.313(5)

is reported in the previous literatures (e.g., Galli and Alberti, 1969; Yoshiasa and Matsumoto, 1985; Allmann and Donnay, 1973). The cell dimensions were determined by a least-square method using 69 reflections. The results are a=8.884(3), b=5.899(4), c=19.292(6) Å and β=97.49(3)°. In the calculation, errors of inclination angles were not considered.

A set of 113 crystallographically independent reflections were used for the structure refinement using the full-matrix least-square program RFINE2 (Finger, 1969). Scattering factors of neutral atoms were taken from *International Tables for X-ray Crystallography,* Vol. IV (1974). Anomalous dispersion corrections were made for all atoms using factors taken from Sasaki (1989). The refinement was initiated with the positional parameters reported by Yoshiasa and Matsumoto (1985). The W- and Z-sites were assigned to be occupied only by Ca and Si, respectively. The X- and Y-sites were assigned to be occupied by Al and Fe with variable occupancy ratio. The overall temperature parameter (B) was employed, because each temperature parameter has strong correlation and relatively larger standard deviation. The final B value is 0.7(2) Å^{-2}. The final R value is 0.088. The obtained positional parameters are listed in Table 3. The cation-anion interatomic distances are given in Table 4.

3. Result and Discussion

The chemical composition of Iwakake pumpellyite varies widely from Fe-rich to Al-rich faces (Fig. 1). Microscopic observation and chemical analysis on a thin section shows that crystal size becomes smaller with the increase of Fe content. The crystal used is an Al-rich one in the specimens of the Iwakake pumpellyite. In the present experiment, enough reflec-

TABLE 4. Interatomic distances (Å) in cation coordination polyhedra

Ca(1) - O(2)$_{\times 2}$	2.42(7)	Si(1) - O(1)$_{\times 2}$	1.55(8)
O(3)$_{\times 2}$	2.32(7)	O(4)	1.65(9)
O (4)	2.39(8)	O(8)	1.69(9)
O (8)	2.54(8)		
O(11)	2.40(10)	mean	1.61
mean	2.40	Si(2) -O(2)$_{\times 2}$	1.54(7)
		O (8)	1.66(8)
Ca(2) - O(1)$_{\times 2}$	2.43(7)	O(10)	1.74(9)
O(2)$_{\times 2}$	2.44(7)		
O(6)	2.87(11)	mean	1.62
O(9)	2.64(10)		
O(10)	2.41(7)	Si(3) -O(3)$_{\times 2}$	1.67(8)
		O(6)	1.77(10)
mean	2.52	O(9)	1.68(11)
X - O(2)$_{\times 2}$	2.07(4)	mean	1.70
O(9)$_{\times 2}$	1.99(7)		
O(11)$_{\times 2}$	1.91(6)		
mean	1.99		
Y - O(1)	1.83(5)		
O(3)	1.95(5)		
O(4)	2.05(7)		
O(5)	1.93(7)		
O(6)	1.95(7)		
O(7)	1.91(7)		
mean	1.94		

tion for the precise analysis of the crystal structure could not be collected because of a crystalline quality problem. The cell volume obtained is larger than that estimated by a relation between total Fe content and cell volume which was proposed by Passaglia and Gottardi (1973).

Figure 3 shows the pumpellyite structure perpendicular to [010]. In the pumpellyite structure, substitution of cations are various in the octahedral X- and Y-sites. For the Iwakake pumpellyite, considerable elements can be restricted to Al, Fe and Mg. The site population refinement shows that Fe distribute both in X- and Y-sites. Therefore, the occupancy factors of Fe for these sites are needed to be constrained so as to satisfy the chemical composition (Mg is regarded as Al). The obtained occupancy ratios of Fe for the X- and Y-sites are 24% and 18%, respectively, that is, 40% and 60% of total Fe distributes in the X- and Y-sites, respectively.

Artioli and Geiger (1994) concluded

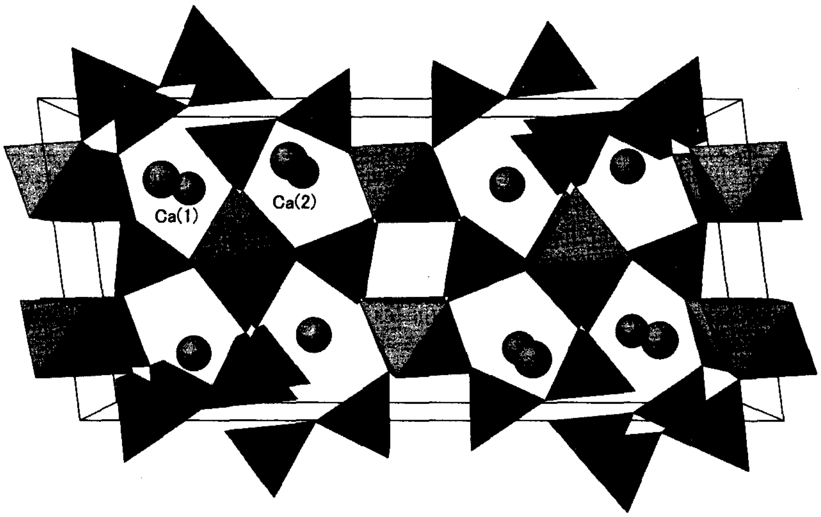

FIG. 3. Pumpellyite structure perpendicular to [010]. The linkage of tetrahedra and octahedra are illustrated. Spheres represent Ca atoms.

that Fe^{2+} and Fe^{3+} are distributed in the X- and Y-sites, respectively. However Akasaka et al. (1997) reported that Fe is distributed essentially in the X-site: Fe^{2+} preferentially occupies the X-site; Fe^{3+} is distributed in the both sites, although it primarily occupies the X-site. The previous studies of single crystal refinement of Al-pumpellyite (Galli and Alberti, 1969; Yoshiasa and Matsumoto, 1985) revealed that Fe occupies only the X-site. Present result of the occupancy ratio shows that the Y-site is abundant with Fe in comparison with that of Fe-pumpellyites reported by Akasaka et al. (1997). Although the ionic valence of Fe is not determined in this study, the distribution of Fe can reasonably be explained assuming that the content of Fe^{2+} in the examined pumpellyite is relatively poor. The cation-oxygen interatomic distances indicate that the space of X-site is larger than that of Y-site (Table. 4). The Mg ions will preferentially occupy the X-site from the consideration of interatomic distances. The occupancy ratios of Mg, Al and Fe of the X-site are 21%, 55% and 24%, respectively. The distribution of Fe^{3+} and Al^{3+} between the X- and Y-sites may depend on the phase formation condition such as a pressure.

Acknowledgments-The authors acknowledge to the late Dr. Kin-ichi Sakurai for providing the investigated specimen. Special thanks are due to Dr. Akira Kato of the National Science Museum, Tokyo, Japan for providing the specimen in the same locality together with occurrence, and to Dr. Kenji Hagiya of the Himeji Institute of Technology for helpful advice about the experimental technique. Thanks are also due to Mr. Y. Shibata, the Instrument Center for Chemical Analysis, Hiroshima University for the chemical analysis by XMA. This work was performed under the approval of the Photon Factory Program Advisory Committee (proposal No. 94P017).

References

AKASAKA, M., KIMURA, Y., OMORI, Y., SAKAKIBARA, M., SHINNO, I. and TOGARI, K. (1997) ^{57}Fe Mössbauer study of pumpellyite-okhotskite- julgoldite series minerals. *Mineral. Petrol.*, **61**, 181–198.

ALLMANN, R. and DONNAY, G. (1973) The crystal structure of julgoldite. *Mineral. Mag.*, **39**, 271–281

ARTIOLI, G. and GEIGER, C. A. (1994) The crystal chemistry of pumpellyite: an X-ray Rietveld refinement and ^{57}Fe Mössbauer study. *Phys. Chem. Minerals*, **20**, 443–453.

FINGER, L. W. (1969) Determination of cation distribution by least-squares refinement of single-crystal X-ray data. *C. I. W. Year Book*, **67**, 216–217.

GALLI, E. and ALBERTI, A. (1969) On the crystal structure of pumpellyite. *Acta Cryst.*, **B25**, 2276–2281.

GOTTARDI, G. (1965) Die Kristallstruktur von Pumpellyit. *Tschermaks Min. Petr. Mitt.*, **10**, 115–119.

International Tables for X-ray Crystallography, Vol. II (1967) Kynoch Press, Birmingham, England.

International Tables for X-ray Crystallography, Vol. IV (1974) Kynoch Press, Birmingham, England.

MOORE, P. B. (1971) Julgoldite, the Fe^{2+} - Fe^{3+} dominant pumpellyite. *Lithos*, **4**, 93–99.

PASSAGLIA, E. and GOTTARDI, G. (1973) Crystal chemistry and nomenclature of pumpellyites and julgoldites. *Can. Mineral.*, **12**, 219–223.

SASAKI, S. (1989) Numerical Tables of Anomalous Scattering Factors Calculated by the Cromer and Liberman's Method, *KEK Report*, **88-14**, 1–136

YOSHIASA, A. and MATSUMOTO, T. (1985) Crystal structure refinement and crystal chemistry of pumpellyite. *Ame. Mineral.*, **70**, 1011–1019.

Received April 13, 1999; accepted September 28, 1999